Diameter Oscillation of Axonemes in Sea-Urchin Sperm Flagella

Hajime M. Sakakibara,* Yuki Kunioka,† Takenori Yamada,† and Shinji Kamimura*
*Department of Life Sciences, Graduate School of Arts and Sciences, the University of Tokyo, Komaba, Meguro, Tokyo, Japan; and
†Section of Biophysics, Department of Physics, Faculty of Sciences, Tokyo University of Science, Kagurazaka, Tokyo, Japan

ABSTRACT The 9 + 2 configuration of axonemes is one of the most conserved structures of eukaryotic organelles. Evidence so far has confirmed that bending of cilia and flagella is the result of active sliding of microtubules induced by dynein arms. If the conformational change of dynein motors, which would be a key step of force generation, is occurring in a three-dimensional manner, we can easily expect that the microtubule sliding should contain some transverse component, i.e., a motion in a direction at a right angle to the longitudinal axis of axonemes. Using a modified technique of atomic force microscopy, we found such transverse motion is actually occurring in an oscillatory manner when the axonemes of sea-urchin sperm flagella were adhered onto glass substrates. The motion was adenosine triphosphate-dependent and the observed frequency of oscillation was similar to that of oscillatory sliding of microtubules that had been shown to reflect the physiological activity of dynein arms (S. Kamimura and R. Kamiya. 1989. *Nature*. 340:476–478; 1992. *J. Cell Biol*. 116:1443–1454). Maximal amplitude of the diameter oscillation was around 10 nm, which was within a range of morphological change observed with electron microscopy (F. D. Warner. 1978. *J. Cell Biol*. 77:R19–R26; N. C. Zanetti, D. R. Mitchell, and F. D. Warner. 1979. *J. Cell Biol*. 80:573–588).

INTRODUCTION

Axonemes of eukaryotic flagella and cilia are composed of a specific 9 + 2 structure enveloped in cell membrane. Our conventional understanding of the sliding microtubule model (Satir, 1968) is that dynein arms on peripheral doublet microtubules generate forces of longitudinal sliding (Summers and Gibbons, 1971) in a base-to-tip direction (Sale and Satir, 1977) during adenosine triphosphate (ATP) hydrolysis, and that the sliding activity regulated in a space- and time-dependent manner is converted into bending motion of the axonemal shaft (Shingyoji et al., 1977; Brokaw, 1989). The main motion we assume here is the longitudinal shearing between peripheral doublet microtubules, freely to some extent but fixed in a 9 + 2 cross-sectional frame.

Compared with other types of motor proteins, such as myosin and kinesin, dynein shows a peculiar feature, oscillatory sliding with high frequency under a certain loaded condition. Such a phenomenon was first described as the nanometer-scale oscillation of microbeads attached on demembranated sea-urchin sperm flagella (Kamimura and Kamiya, 1989). The observed frequency was 300–450 Hz at 1.0 mM of ATP and was revealed to be due to the back-and-forth small sliding of microtubules with amplitudes reflecting the unit size of tubulin dimers (Kamimura and Kamiya, 1992). The same activity was also shown in the flagella of wild-type *Chlamydomonas reinhardtii* as well as outer-armless or spokeless mutants (Yagi et al., 1994). Therefore, such oscillatory behavior of axonemes would be caused by the common but specific chemomechanical properties of axonemal dyneins. The oscillatory motion can occur without any cooperative interactions among multiple dynein arms, since a similar type of motion was observed in the case of a solitary dynein arm on extruded doublet microtubule interacting with a bovine brain singlet microtubule (Shingyoji et al., 1998) with a frequency almost comparable to the activity of inner arm components (Yagi et al., 1994).

This study was carried out to clarify the detailed features of oscillatory motion using atomic force microscopy (AFM). So far, the oscillatory motion has been detected as nanometer-scale displacement of microbeads (Kamimura and Kamiya, 1989, 1992; Yagi et al., 1994) or glass microneedles (Tani and Kamimura, 1999; Shingyoji et al., 1998) placed on axonemes under conventional optical microscopes. Such techniques can provide us with only the information of microtubule displacement in a plane vertical to the optical axis. Therefore, the detailed and local properties of the motion, for example, the motion in a direction of axonemal diameter and the local variation of dynein arm activity, have been obscured.

AFM has been developed as a new application of the technique of scanning tunneling microscopy (Binnig et al., 1983, 1986). By scanning the surface of specimens with a fine silicon probe placed on the end of a cantilever and by detecting its small displacement with an amplifying technique using optical levers, we can collect the information of specimen height (z-position) on a scale of nanometers or angstroms. The technique to observe in aqueous solutions has been already established (Marti et al., 1987; Henderson et al., 1992). In addition to the main applications of AFM focusing on structural studies, there were several reports that described the mechanical properties of molecules, e.g., biotin-streptavidin interaction (Lee et al., 1994), dextran elongation (Rief et al., 1997), and protein folding (Carrion-Vazquez et al., 1999; Rief et al., 1999), as well as the elastic

Submitted May 21, 2003, and accepted for publication August 27, 2003.

Address reprint requests to Shinji Kamimura, Dept. of Life Sciences, Graduate School of Arts and Sciences, the University of Tokyo, Komaba 3-8-1, Meguro, Tokyo 153-8902, Japan. Tel.: +81-3-5454-6665; Fax: +81-3-5454-6998; E-mail: kam@nano.c.u-tokyo.ac.jp.

0006-3495/04/01/346/07 $2.00

properties of biological materials (Henderson et al., 1992; Vinckier et al., 1996; Yoshikawa et al., 1999; Kis et al., 2002). These studies indicate that by specific modifications of the techniques, AFM can be utilized to study the physical properties of molecules in more broad fields of study. This report is the first example to apply the AFM technique to analyze active organelle motility. Another point to be stressed is that we simultaneously measured the LFM (lateral force microscopy) signals reflecting lateral twisting of cantilevers. So far, the LFM signals had been used to get information about the magnitude of surface friction (Mate et al., 1987). The same signals were used here to obtain a parameter indicating the active displacement of specimen parallel to substrate surfaces, which is microtubule sliding or lateral undulation of flagella under the present experimental conditions. In contrast, the conventional AFM signals indicate the motion of axonemes vertical to the substrate, which corresponding to the radial expanding or shrinking of axonemes.

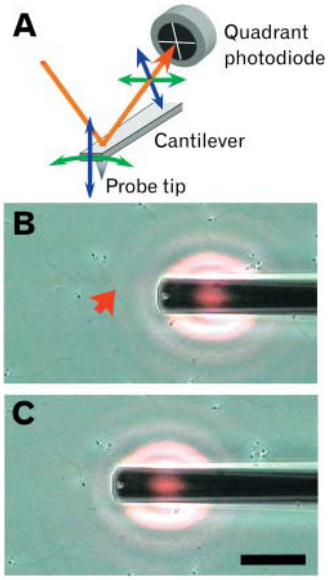

FIGURE 1 (*A*) A schematic drawing illustrating the L- motion (*green*) and V-motion (*blue*) of the cantilever. The orange line indicates the laser-beam path for the detection of cantilever deflection. (*B* and *C*) Photographs showing a cantilever tip and flagella of sea urchin spermatozoa. The area where the laser beam illuminated the cantilever appears red. (*B*) The cantilever (OMCL-RC800PSA) was first placed near the specimen locus to measure (*short red arrow*). (*C*) The cantilever tip was then driven by piezo-actuator toward the specimen. Scale bar, 50 μm. During signal recording the lamp for the microscope illumination was turned off.

MATERIALS AND METHODS

Preparation of demembranated sperm flagella

Dry sperm was collected from sea urchins (*Hemicentrotus pulcherrimus*, *Pseudocentrotus depressus*, or *Anthocidaris crassispina*) by injecting ~0.1 ml natural seawater containing 10 mM acetylcholine into male body cavities. The collected dry sperm was stored in a refrigerated test tube before experiments.

Spermatozoa were demembranated as described by Gibbons and Gibbons (1972), with some modifications. Dry sperm (1 μl) were first suspended in 10 μl filtered natural seawater. The suspension was then mixed with 300 μl extracting solution containing 200 mM K-acetate, 2 mM $MgCl_2$, 0.5 mM EGTA, 0.1 mM EDTA, 10 mM Tris-HCl, pH 8.3, 0.04% (w/v) Triton-X100, and 1 mM dithiothreitol. The mixture was swirled and kept for 30–60 s on ice. The demembranation was ceased by adding 1000 μl reactivation solution (200 mM K-acetate, 2 mM $MgCl_2$, 0.5 mM EGTA, 0.1 mM EDTA, 20 mM Tris-HCl, pH 8.3 and 1 mM dithiothreitol).

A 3-μl aliquot of the resultant suspension of demembranated sperm flagella was introduced into a chamber made of silicon rubber sheet (28 × 28 mm^2, 3-mm thickness, with 20 × 20 mm^2 cut made in the center) placed on a coverslip (54 × 28 mm^2). The coverslip had been previously treated with 2% aqueous solution of 3-aminopropylteiethoxysilane (Shin-Etsu Chemical, Tokyo, Japan) for 2 min to make the glass surface positively charged. This makes coverslip surfaces adsorptive for demembranated axonemes. Reactivating solution (30 μl) containing 1.0 mM ATP was then added onto the specimen and stayed for 5 min. This procedure was done to release spermatozoa that were loosely attached on the glass surface. After perfusing with ATP-free reactivating solution to wash, 1300 μl reactivating solution (with various ATP concentrations) was added. The medium condition was the same as those for the reactivation of flagellar beats, but here we could not observe any apparent motion of flagella since the sperm heads and almost all of the lengths of flagellar shafts were immobilized by being adhered on the glass surface. The specimen was observed with AFM (NV2500, Olympus, Tokyo, Japan) equipped with an inverted phase-contrast microscope (IX-70 with LCAch ×20 PhC; Olympus) at room temperature (25–28°C).

AFM set-up

Cantilevers with different compliances, i.e., triangular OMCL-TR400PSA (20 pN nm^{-1} of compliance, 20 nm of tip-curvature, 11 kHz of resonant frequency, and 200 μm in length; Olympus), or rectangular OMCL-RC800PSA (50 pN nm^{-1}, 20 nm, 18 kHz, and 200 μm; Olympus) and BL-RC150VB (6 pN nm^{-1}, 40 nm, 13 kHz, and 100 μm; Olympus) were used. Their resonant frequencies in water were above 3000 Hz. In this study, we determined the vertical motion of cantilevers (*z*-position) as well as their twisting motion (Fig. 1 *A*). The vertical motion has been used for the conventional AFM imaging of surface height. It indicates the specimen motion in a direction at a right angle to the longitudinal axis of flagella, which is denoted as V-motion here. So we expected the V-motion signals to represent the motion occurring in the direction of axonemal diameter. The magnitude of 100 mV in the V-motion signal corresponds to 20 nm of vertical displacement. The twisting motion of the cantilever was simultaneously detected as a laser beam deflection in a direction at a right angle to that for the AFM signal on a quadrant photodetector. It corresponds to the lateral motion of the probe tip in a direction parallel to the coverslip surface (denoted as L-motion here). The L-motion signals gave us only relative values and did not always represent the direct magnitude of motion since the possibility that probe tips would slip laterally on specimens could not be ruled out.

Procedures to record V- and L-motion signals

Phase contrast images of flagellar axonemes placed on a coverslip surface in the chamber were observed with a CCD camera (CS5110C, Tokyo Electric Industry, Tokyo, Japan). The CCD camera was also used to find out the appropriate centering position of the laser beam for the V-/L-motion signals. Illumination with a halogen-tungsten lamp for the video images was turned off during signal recording of V-/L-motions.

For the measurement of signals, an axoneme was first placed near the tip of the cantilever within a working area of the piezo-actuator of AFM (Fig. 1 *B*). The height of the cantilever was manually manipulated to access the

glass substratum avoiding direct contact. The cantilever was then driven with the piezo-actuator toward the axoneme until we could detect any V- and L-motion signals reflecting tip-contact with the specimen (Fig. 1 *C*). When no oscillatory motion was detected, the cantilever tip was withdrawn upward several micrometers off the glass surface and displaced by 40 nm in the direction of the cantilever tip. Then the cantilever was moved toward the specimen again. These procedures were repeated several times until the cantilever tip was apparently moved beyond the specimen. Under the present experimental condition, we have chosen straight axonemes immobilized on a glass surface as shown in Fig. 1 *B*.

When we detected any signals indicating the cantilever oscillation in either V- or L-motion, they were amplified (gain ×10 with a frequency band of 10–3000 Hz) and recorded on a computer through a USB digital audio processor (SE-U77, Onkyo, Tokyo, Japan) using software for sound-recording (DigiOnSound, Digion, Tokyo, Japan; sampling frequency was 44.1 kHz). The recording and amplifying system had flat spectral properties within the frequency range used for the present study. Our system contained both mechanical noise derived from the vibration of the laboratory floor and electric noise probably derived from feedback-loop circuits included in the AFM apparatus. Such noise, usually within a range of 50–100 Hz, could not be eliminated completely. The resonant vibration of cantilevers also produced noise. However, these noises were easily distinguished from the signals representing axonemal oscillation by both the spectral shape and frequency values. After recording the signals, phase-contrast microscope images were recorded on videotapes, from which further detailed analysis of the angle between cantilever and axoneme was executed.

In this study, ATP dependency of the frequency was first investigated, which gave direct evidence indicating that the signals we detected were representing active motion occurring in the axonemes. For the experiment, oscillation was measured at 0.2 mM ATP at first, and then 500 μl of 3.1 mM ATP was added into the chamber to get the final concentration of 1.0 mM ATP. Other experiments to measure oscillatory frequency were carried out at 0.5 mM ATP.

Data analysis

Recorded signals were played back and analyzed with a fast Fourier transform (FFT) analyzer. Detailed analysis of the time course of oscillatory frequency was executed with shareware FFT program (FFT Wave, E.N.Software, Tokyo, Japan) after converting the recorded signals into WAV format. FFT was also carried out with an FFT analyzer (CF-5220, Ono Sokki, Tokyo, Japan). Auto- and cross-correlations of signals were calculated using ASC code data converted from recorded signals.

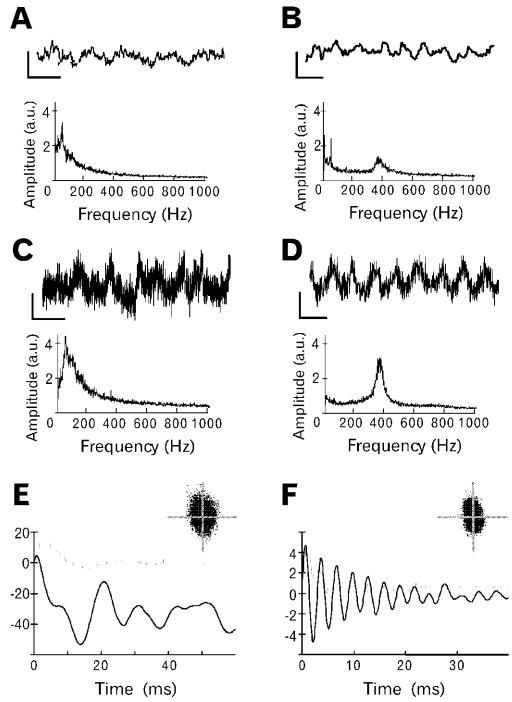

FIGURE 2 A typical example showing the oscillatory V- and L-motion of the cantilever on a sea urchin (*P. depressus*) sperm flagellum. The left (*A*, *C*, *E*) and right (*B*, *D*, *F*) columns are the data obtained at 0.2 and 1.0 mM ATP, respectively. *A* and *B*, and *C* and *D* are the data showing V- and L-motion of the cantilever, respectively. The top trace in each figure shows the time course of recorded signals. Vertical scales indicate 100 mV. In the case of V-motion signals (*A* and *B*), 100 mV corresponds to 20 nm. Horizontal scales are 20 and 3.3 ms in *A* and *C* and *B* and *D*, respectively. Amplitude (with an arbitrary unit) spectrum obtained with FFT is also shown in each figure. FFT spectra were calculated from 8000 points of data recorded at 1000-Hz sampling frequency. The main peaks are at 46 (*A*), 365 (*B*), 48 (*C*) and 360 (*D*) Hz, respectively. *E* and *F* show the results showing correlation between V- and L-motion signals. Auto-correlation of V-motion signals (*hatched line*) and cross-correlation between V- and L-motion signals (*thick line*) are shown. Ordinates are of arbitrary units by putting the calculated value as 1.0 when the time is zero. Insets are the plots of V-motion (abscissas) and L-motion (ordinates) for the 8000 data. Axis bars correspond to 200 mV. Correlation coefficients are −0.0955 and −0.2920 in *E* and *F*, respectively.

RESULTS

ATP dependency of the oscillatory motion of axonemes

First, we tested how the oscillation frequency depended on ATP concentration because it would provide the most reliable criteria to know that we were actually detecting some ATP-dependent activity of axonemes. Fig. 2 shows the data of V- and L-motion signals at 0.2 or 1.0 mM ATP. Results of FFT and correlation analysis of the observed signals are also shown. The observed ATP dependency was almost consistent with the Km (94 μM MgATP) and Vm (340 Hz) values reported by Kamimura and Kamiya (1989). It indicates that we were detecting the same type of active oscillation of microtubules with AFM as had been shown with optical microscopy methods. The amplitude of the V-motion varied usually within a range of 10 nm. The corresponding maximal forces (500 pN) estimated by cantilever compliance (20–50 pN nm^{-1}) were smaller than or within the range of sliding forces that had been detected with glass microneedle techniques (Tani and Kamimura, 1999). The maximal forces were not dependent on the compliance of cantilevers we used. Therefore, it is likely that cantilever deflection was not the result of force balancing between cantilever elasticity and forces exerted by axonemes. Fig. 2 shows a typical case where both V- and L-motion signals show the oscillation with the same frequency. Although the plot of V- versus L-motion signals does not show clear correlation due to the noise, the cross-correlation analysis indicates that the motions were almost synchronized in phase (Fig. 2, *E–F*). As stated below in more detail, both V- and L-motion signals were not always detected simultaneously.

Comparison between V- and L-motion signals

In ~40% cases, both V- and L-motion signals showed oscillatory motions with the same frequencies as shown in Fig. 2. In many other cases, only V-motion signals were recorded. Since the L-motion signals are reflecting the motion in a direction parallel to the glass surface and doublet microtubules are sliding in an oscillatory manner along the axonemal axis, we can expect that there should be some dependency of recorded signals on the angles between cantilever and axonemes. Fig. 3 shows how the frequency to observe oscillatory V- and/or L-motion signals depended on angles. In 35 and 98% of cases when we detected any oscillatory signals, they were observed as L- and V-motions, respectively. The L-motion signals were detected most frequently when the cantilever was placed at a right angle to the axonemal axis. We did not collect data at around 180° because we avoided mechanical obstruction between sperm heads and cantilevers. No L-motion signals could be detected at the angle around 0° ($n = 12$). It indicates that the detected L-motion signals reflected the oscillatory sliding of microtubules occurring in the longitudinal direction of axonemes. On the other hand, the V-motion signals were detected in almost all cases, independently of the angle to the axonemal axis.

Distribution of oscillatory V-motion frequencies

AFM also helped us to collect frequency data at narrow restricted areas along axonemes, which may reflect a difference in local activity of dynein arms. Accumulated V-motion data at 0.5 mM ATP are shown in Fig. 4. The observed frequency was ranged from 130 to 860 Hz. A major peak was located at around 190–690 Hz (320 ± 99 Hz, $n = 108$), the mean value of which was almost the same reported previously with the optical technique of nanometry using microbeads (Kamimura and Kamiya, 1989, 1992). However, a smaller peak around 150–210 Hz (180 ± 14 Hz, $n = 18$) was also evident that was not detected using the previous optical techniques. Oscillatory signals with lower frequency tended to be detected more frequently using more compliant cantilevers (BL-RC150VB of 6 pN nm^{-1}), but we found no positive correlation of the measured frequency with other experimental conditions, i.e., the angles between cantilever and axonemes and the cantilever position along axonemes.

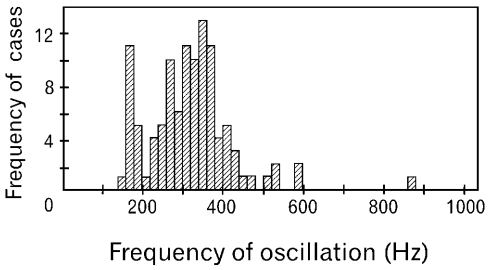

FIGURE 4 Histogram showing the frequency distribution of the V-motion signals obtained with flagellar axonemes of sea urchin (*A. crassispina*) spermatozoa at 0.5 mM ATP. The mean value of all is 320 ± 99 Hz ($n = 108$). Two peaks of 180 ± 14 Hz ($n = 18$) and 350 ± 83 Hz ($n = 91$) are evident.

We found many cases of oscillations having both lower and higher frequencies simultaneously. In some cases, the oscillation with the higher frequency corresponded to a harmonic motion of the lower frequency. The other cases we found showed oscillatory signals with two independent frequencies. A typical case is shown in Fig. 5. Some fluctuations of oscillatory frequency as shown in Fig. 5 *A* were usually found under our experimental conditions. It may imply that there exist some temporal variations of dynein activities, although some of them would have come from the instability of our long recording techniques. We could not find out any consistent data showing the correlation of such patterns of frequency in the spectrum of oscillation with our experimental conditions.

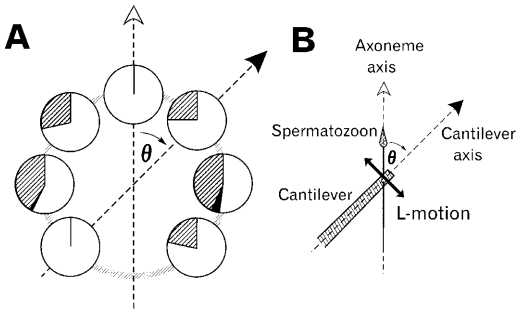

FIGURE 3 (*A*) Circle graphs showing the relationship between the cantilever angle (divided by 45° range) to the axoneme and the frequency of recorded oscillatory signals at 0.5 mM ATP. The results of 311 cases of *A. crassispina* spermatozoa with cantilever OMCL-TR400PSA and 141 cases of *H. pulcherrimus* spermatozoa with OMCL-RC800PSA are combined. The angle, θ, is as illustrated in *B*. White, black, and shaded areas in circle graphs represent the cases when only V-motion, only L-motion, and both of them, respectively, are recorded. The number of data included in each circle graph clockwise from the left bottom is 5, 152, 83, 12, 85, 87, and 28 (total $n = 452$) at −135°, −90°, −45°, 0°, +45°, +90°, and +135° of θ, respectively. L-motion was most frequently observed at around $\theta = \pm 90°$ ($p < 0.001$, Fisher's exact test).

DISCUSSION

Previous studies have revealed that axonemal microtubules showed oscillatory sliding under the condition where the free bending of axonemes was restricted by adhering them on glass surfaces (Kamimura and Kamiya, 1989, 1992; Yagi et al., 1994). The observed frequency was at around 350 Hz with 1.0 mM ATP. Such motion was detected by measuring the fine displacement of microbeads attached on axonemes. Due to the restriction of microscopy in such previous studies, only two-dimensional displacements could be analyzed. With the modified technique of AFM presented here, we were able to detect the motion in the direction parallel to the optical axis

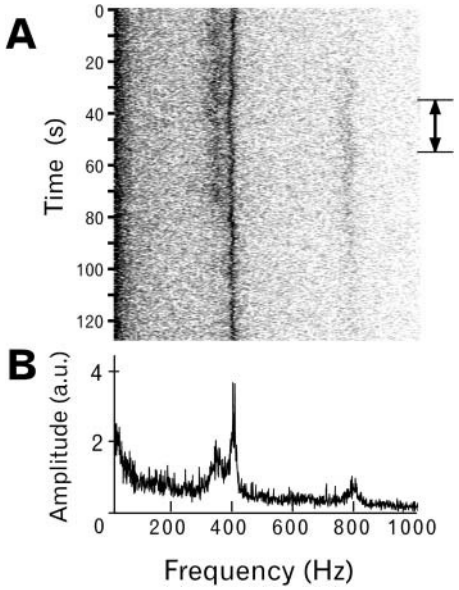

FIGURE 5 An example of oscillation showing two different frequencies. *A* indicates a frequency time chart of recorded V-motion signals at 0.5 mM ATP. There are evident three frequency peaks. The peak at the highest frequency (809 Hz) corresponds to the doubled one of the second (407 Hz). The third peak is the oscillation at around 350 Hz that fluctuated and disappeared completely during recording. *B* is the amplitude spectrum (with an arbitrary unit) of data during the period indicated by the arrow in *A*.

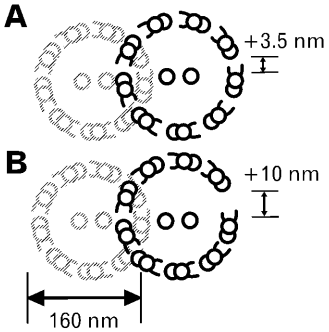

FIGURE 6 A schematic drawing illustrating the two tentative patterns of 10 nm (6%) change of axonemal diameter. The hatched 9 + 2 structure shows the original size of axoneme with 160 nm of diameter. (*A*) A case where the uniform expanding of interdoublet spacing (3.5 nm, 17%) is occurring. (*B*) A case where the diameter change of the axoneme is derived from the expanding of interdoublet spacing (10 nm, 50%) at a specific site. Central-pair microtubules are shown with a tentative orientation that could not be defined in this study.

(V-motion) as well as that in the optical planes (L-motion). This is one of the major advantages of this technique.

Both L- and V-motion signals were detected simultaneously in many cases, so we could analyze how the detected signals were dependent on the angles between the cantilever and the axoneme (Fig. 3). The L-motion was detected most frequently when the cantilever was placed at a right angle ($\theta = \pm 90^{\circ}$). Thus, the L-motion of cantilever in this case should reflect microtubule sliding in the longitudinal direction of the axoneme, as expected from our conventional comprehension of the sliding activity of dynein arms. The sliding microtubule model of flagella implies nothing about the radial motion of axonemes. However, V-motion signals were detected unexpectedly frequently with the present technique, in 98% of cases in which any oscillatory signals were detected. This represented 30–80% of all our experimental trials. Our observation of V-motion signals reveals a novel feature of axonemal motility, i.e., sea-urchin sperm flagella also oscillate in the direction of axonemal diameter. Although the biophysical meaning of the high-frequency longitudinal oscillation of axonemes is still not clear, our observation suggests that the spacing between peripheral doublet microtubules is not always fixed, but varies during the cross-bridge cycles of dynein arms.

The 10 nm of V-motion, the maximal amplitude we observed, corresponds to an ~6% change of axonemal diameter. If the motion is derived from the uniform expansion of axonemes, it indicates a 3.5-nm increase of interdoublet spacing on average (Fig. 6 *A*). Putting the width of doublet microtubules and the interdoublet spacing at 35 and 21 nm, respectively, we can assume there is a 17% mean increase of interdoublet spacing. Another extreme case, that a 10-nm change of spacing (50% increase) is occurring at a specific interdoublet site of axoneme, may be also possible (Fig. 6 *B*). The range of diameter expansion was within those shown by electron microscopy observations, where different interdoublet spacing was observed depending on the medium conditions of bication (Warner, 1978; Zanetti et al., 1979). In those studies, the physiological meaning of such diameter variation has long been unclear and the possibility of some artificial effects during chemical fixation for electron microscopy could not be excluded. Our observation clearly revealed that the 9 + 2 configuration of axonemes is not always rigid and fixed, and the spacing between doublet microtubules would be flexibly varied depending on the physiological states of dynein arms. The change of interdoublet spacing of 3.5 nm on average is within a range of reported conformational change of dynein molecules (Burgess et al., 2003). The transverse component of dynein arm motion, in other words, conformational changes of dynein molecules to push or to pull adjacent microtubules, is a new feature of the axonemal motility that should be added to well-known longitudinal power-strokes for microtubule sliding. This is the first evidence suggesting that a three-dimensional conformation change of dynein motors is occurring.

A crucial point to be solved when we get more insight into the beating mechanism of axonemes is how the three-dimensional arrangement of axonemal components, e.g., dynein arms, spoke heads (Wargo and Smith, 2003), and central pair (Omoto and Kung, 1979), is organized during flagellar beatings. The intermolecular distance of these components in bending axonemes should be described in

more detail for our further understanding of the flagellar motility. Additionally, careful assumptions of interdoublet spacing are required when we estimate the exact magnitude of sliding distance of doublet microtubules from the bend angle of axonemes. In many previous studies, we simply assumed that the interdoublet spacing should be fixed without any evidence. Our data suggest such estimates of sliding distance would have some errors of up to 17–50%. Furthermore, the change of interdoublet spacing should affect the magnitude of torques generated by, or that of resistant loads given to, dynein arms. Therefore, the change of interdoublet spacing could modify mechanical stresses on dynein arms at work. The evidence presented here implies that we need to consider such dynamic change of interdoublet spacing (Lindemann and Kanous, 1997; Lindemann, 2003) for further understanding of axonemal mechanics and regulatory mechanisms of flagellar motility.

Another point to be noted here is the two peaks in the frequency distribution of detected oscillation (Fig. 4). There would be two different explanations. From biochemical studies of *Tetrahymena* dynein (Omoto and Johnson, 1986; Shimizu et al., 1989) it was assumed that the maximal rate of ATP turnover by dynein outer arms could be around 150 s^{-1}, an estimated maximal rate of conversion from dynein-ATP to dynein-ADP/Pi. Thus, one possibility is that the oscillation with lower frequency (180 $\pm$ 14 Hz) comes from the motion of dynein arms functioning with this rate of ATP turnover, the base frequency. In this case, however, an additional mechanism is required to explain why the low frequency oscillation has no longitudinal component as detected by the optical methods and how the cooperative motion among dynein arms can generate higher frequency oscillation of 350 $\pm$ 83 Hz. A second possibility is that 180 $\pm$ 14 Hz signals would reflect the activity of inner dynein arms that is usually obscured with outer-arm activity because outer-arm depleted axonemes had from one-third to one-half the values of oscillatory frequencies of intact ones (Yagi et al., 1994; Shingyoji et al., 1998).

Studies so far show no direct evidence saying how the variation of oscillatory frequency as shown in Figs. 4 and 5 depends on the sites along axonemes. In the case of oscillatory longitudinal sliding, we can assume that some doublet microtubules are moving in unison as has been revealed by the cross-correlation analysis of microbead motions at two different sites along axonemes (Kamimura and Kamiya, 1992). When the diameter oscillation occurs concomitantly with the longitudinal oscillation, we may expect that there is little local variation of oscillatory frequency in the case of straightened axonemes as we observed in this study. It brings us to another question, whether the neck region of a flagellar axoneme with a basal body could make some mechanical hindrance to microtubules sliding. However, the oscillatory motion does not seem to be directly hindered by the existence of sperm heads (Kamimura and Kamiya, 1989). It may imply some mechanical flexibility of the basal body structure against deformation in nanometer scales (Brokaw, 1991). Another crucial point to be investigated is how the high-frequency oscillation depends on axonemal bends, since bending-curvature has been assumed as a key parameter in the regulatory mechanism of dynein arm activity (Brokaw, 1971, 2002; Lindemann, 2003). Further detailed investigations with both optical and AFM techniques should be awaited to know more precise features of oscillatory behavior of dynein arms.

This work was supported by Grant-in-Aid for Scientific Research (B) 13450096 from Japan Society for the Promotion of Science.

REFERENCES

Binnig, G., C. F. Quate, and C. Gerber. 1986. Atomic force microscope. *Phys. Rev. Lett.* 56:930–933.

Binnig, G., H. Rohrer, C. Gerber, and E. Weibel. 1983. 7×7 Reconstruction on Si(111) resolved in real space. *Phys. Rev. Lett.* 50:120–123.

Brokaw, C. J. 1971. Bend propagation by a sliding filament model for flagella. *J. Exp. Biol.* 55:289–304.

Brokaw, C. J. 1989. Direct measurement of sliding between outer doublet microtubules in swimming sea urchin sperm flagella. *Science.* 243:1593–1596.

Brokaw, C. J. 1991. Microtubule sliding in swimming sperm flagella – direct and indirect measurements on sea-urchin and tunicate spermatozoa. *J. Cell Biol.* 114:1201–1215.

Brokaw, C. J. 2002. Computer simulation of flagellar movement VIII: Coordination of dynein by local curvature control can generate helical bending waves. *Cell Motil. Cytoskeleton.* 53:103–124.

Burgess, S. A., M. L. Walker, H. Sakakibara, P. J. Knight, and K. Oiwa. 2003. Dynein structure and power stroke. *Nature.* 421:715–718.

Carrion-Vazquez, M., A. F. Oberhauser, S. B. Fowler, P. E. Marszalek, S. E. Broedel, J. Clarke, and J. M. Fernandez. 1999. Mechanical and chemical unfolding of a single protein: A comparison. *Proc. Natl. Acad. Sci. USA.* 96:3694–3699.

Gibbons, B. H., and I. R. Gibbons. 1972. Flagellar movement and adenosine triphosphatase activity in sea urchin sperm extracted with Triton X-100. *J. Cell Biol.* 54:337–357.

Henderson, E., P. G. Haydon, and D. S. Sakaguchi. 1992. Actin filament dynamics in living glial cells imaged by atomic force microscopy. *Science.* 257:1944–1946.

Kamimura, S., and R. Kamiya. 1989. High-frequency nanometre-scale vibration in 'quiescent' flagellar axonemes. *Nature.* 340:476–478.

Kamimura, S., and R. Kamiya. 1992. High-frequency vibration in flagellar axonemes with amplitudes reflecting the size of tubulin. *J. Cell Biol.* 116:1443–1454.

Kis, A., S. Kasas, B. Babić, A. J. Kulik, W. Benoît, G. A. D. Briggs, C. Schönenberger, S. Catsicas, and L. Forró. 2002. Nanomechanics of microtubules. *Phys. Rev. Lett.* 89:248101.

Lee, G. U., D. A. Kidwell, and R. J. Colton. 1994. Sensing discrete streptavidin-biotin interactions with atomic force microscopy. *Langmuir.* 10:354–357.

Lindemann, C. B. 2003. Structural-function relationships of the dynein, spokes, and central-pair projections predicted from an analysis of the forces acting within a flagellum. *Biophys. J.* 84:4115–4126.

Lindemann, C. B., and K. S. Kanous. 1997. A model for flagellar motility. *Int. Rev. Cytol.* 173:1–72.

Marti, O., B. Drake, and P. K. Hansma. 1987. Atomic force microscopy of liquid-covered surfaces – atomic resolution images. *Appl. Phys. Lett.* 51:484–486.

Mate, C. M., G. M. McClelland, R. Erlandsson, and S. Chiang. 1987. Atomic-scale friction of a tungsten tip on a graphite surface. *Phys. Rev. Lett.* 59:1942–1945.

Omoto, C. K., and K. A. Johnson. 1986. Activation of the dynein adenosine triphosphatase by microtubules. *Biochemistry.* 25:419–427.

Omoto, C. K., and C. Kung. 1979. The pair of central tubules rotates during ciliary beat of Paramecium. *Nature.* 279:532–534.

Rief, M., F. Oesterhelt, B. Heymann, and H. E. Gaub. 1997. Single molecule force spectroscopy on polysaccharides by atomic force microscopy. *Science.* 275:1295–1297.

Rief, M., J. Pascual, M. Saraste, and H. E. Gaub. 1999. Single molecule force spectroscopy of spectrin repeats: Low unfolding forces in helix bundles. *J. Mol. Biol.* 286:553–561.

Sale, W. S., and P. Satir. 1977. Direction of active sliding of microtubules in *Tetrahymena* cilia. *Proc. Natl. Acad. Sci. USA.* 74:2045–2049.

Satir, P. 1968. Studies on cilia. III. Further studies on the cilium tip and a ''sliding filament'' model of ciliary motility. *J. Cell Biol.* 39:77–94.

Shingyoji, C., H. Higuchi, M. Yoshimura, E. Katayama, and T. Yanagida. 1998. Dynein arms are oscillating force generators. *Nature.* 393:711–714.

Shingyoji, C., A. Murakami, and K. Takahashi. 1977. Local activation of Triton-extracted flagella by ionophoretic application of ATP. *Nature.* 265:269–270.

Shimizu, T., S. P. Marchese-Rogana, and K. A. Johnson. 1989. Activation of the dynein adenosine triphosphatase by cross-linking to microtubules. *Biochemistry.* 28:7016–7021.

Summers, K. E., and I. R. Gibbons. 1971. Adenosine triphosphate-induced sliding of tubules in trypsin-treated flagella of sea urchin sperm. *Proc. Natl. Acad. Sci. USA.* 68:3092–3096.

Tani, T., and S. Kamimura. 1999. Dynein-ADP as a force generating intermediate revealed by a rapid reactivation of flagellar axoneme. *Biophys. J.* 77:1518–1527.

Vinckier, A., C. Dumortier, Y. Engelborghs, and L. Hellemans. 1996. Dynamical and mechanical study of immobilized microtubules with atomic force microscopy. *J. Vac. Sci. Technol. B.* 14:1427–1431.

Wargo, M. J., and E. F. Smith. 2003. Asymmetry of the central apparatus defines the location of active microtubule sliding in *Chlamydomonas* flagella. *Proc. Natl. Acad. Sci. USA.* 100:137–142.

Warner, F. D. 1978. Cation-induced attachment of ciliary dynein cross-bridges. *J. Cell Biol.* 77:R19–R26.

Yagi, T., S. Kamimura, and R. Kamiya. 1994. Nanometer scale vibration in mutant axonemes of Chlamydomonas. *Cell Motil. Cytoskeleton.* 29:177–185.

Yoshikawa, Y., T. Yasuike, A. Yagi, and T. Yamada. 1999. Transverse elasticity of myofibrils of rabbit skeletal muscle studied by atomic force microscopy. *Biochem. Biophys. Res. Commun.* 256:13–19.

Zanetti, N. C., D. R. Mitchell, and F. D. Warner. 1979. Effects of divalent cations on dynein cross bridging and ciliary microtubule sliding. *J. Cell Biol.* 80:573–588.